ELSEVIER

International Journal of Solids and Structures 41 (2004) 5717–5731

INTERNATIONAL JOURNAL OF SOLIDS and STRUCTURES

www.elsevier.com/locate/ijsolstr

Dynamic response of active composite plates: shape memory alloy fibers in polymeric/metallic matrices

Rivka Gilat [a,*], Jacob Aboudi [b]

[a] *Faculty of Engineering, Department of Civil Engineering, The College JAS Ariel, Ariel 44837, Israel*
[b] *Faculty of Engineering, Tel Aviv University, Ramat Aviv 69978, Israel*

Received 25 July 2003; received in revised form 29 December 2003
Available online 11 June 2004

Abstract

Micromechanically established constitutive equations for unidirectional composites with shape memory alloy fibers embedded in polymeric or metallic matrices are derived. These equations are subsequently employed to analyze the nonlinear behavior of infinitely wide composite plates that are subjected to the sudden application of thermal loading. The shape memory alloy fibers are activated by a mechanical loading and unloading of the composite to an overall traction-free state (activation), prior to the application of the thermal shock. The present micro-macro-structural approach enables an accurate modelling that accounts for the interaction of shape memory alloy fibers with its surrounding rather than the commonly adopted simplified analyses.

Keywords: Shape memory alloy materials; Micromechanics analysis; Composite materials; Composite structures

1. Introduction

Shape memory alloy (SMA) materials undergo phase transformation which is caused by the application of stress and/or temperature. At high temperatures, the material behavior is nonlinear and hysteretic but yet, yields at the end of a mechanical loading-unloading cycle the original stress–strain-free state (superelastic behavior). At lower temperatures, a mechanical loading-unloading results in a residual deformation which can be recovered by a temperature increase (shape memory effect). The latter effect can be utilized to control the behavior of structures in which SMA materials have been embedded.

Three-dimensional constitutive relations that can model the shape memory behavior have been presented by various investigators, see Boyd and Lagoudas (1994), Auricchio et al. (1997) and Brocca et al. (2002) for example and references cited there. Birman (1997) reviewed various constitutive equations and discussed some applications of SMA materials.

* Corresponding author. Tel.: +972-39248937; fax: +972-39066351.
E-mail address: gilat@eng.tau.ac.il (R. Gilat).

0020-7683/$ - see front matter © 2004 Elsevier Ltd. All rights reserved.
doi:10.1016/j.ijsolstr.2004.04.043

One way of incorporating SMA materials in structures is by embedding SMA fibers in polymeric or metallic matrices to generate active composites. The analysis of such composites should be based on a micromechanical approach in which the detailed interaction between the constituents is accounted for. In the presence of SMA constituents, the micromechanical analysis is necessarily nonlinear and path-dependent. In the presence of metallic materials additional nonlinear effects exist due to their inelastic behavior. Micromechanics modelling of elastic materials with embedded SMA fibers have been presented by Boyd and Lagoudas (1994) and Kawai et al. (1996), whereas micromechanical analysis of elastic-plastic materials with SMA phases has been given by Cherkaoui et al. (2000) and Lagoudas et al. (1996), for example.

The analysis of composite structures that involve embedded SMA materials should be based on constitutive relations that have been established by a micromechanical approach. Alternatively, several investigators adopted a simplified approach according to which the detailed interaction of the SMA material with its surrounding is neglected and its effect, as deduced from the behavior of the monolithic SMA material, is incorporated, see Turner (2000), Lee and Lee (2000) and Tawfik et al. (2002), for example.

In the present paper, the behavior of plates consisting of active composites and subjected to the sudden application of thermal loading is considered. In particular, the response of infinitely wide plates is studied, in the framework of the classical plate theory, in conjunction with von Karman strain–displacement relations. The structural analysis is based on a micromechanically established constitutive relations which, due to the complicated state of stress, strain and temperature resulting from the structural behavior, are used at every point of the plate. Consequently, such an analysis forms a micro-macro-structural approach.

In order to establish the global thermomechanical constitutive law of unidirectional composites consisting of polymeric or metallic matrices and embedded SMA fibers, the so called generalized method of cells micromechanical model (Paley and Aboudi, 1992; Aboudi, 1996) is employed. This micromechanical model takes into account the individual behavior of the various constituents and their detailed interaction. For a detailed explanation of the method see the recent textbook by Herakovich (1998). It should be noted that the generalized method of cells has been implemented into the recently developed micromechanics analysis code MAC/GMC (which does not include, as yet, the capability of SMA modelling that is presented in this paper) which has many user friendly features and significant flexibility (see Bednarcyk and Arnold (2002) for the most recent version of its user guides).

The modelling of Lagoudas et al. (1996) is employed to predict the behavior of the SMA phase. This three-dimensional model is capable of producing the superelastic and the shape memory effects. Two kinds of matrices in which the SMA fibers can be embedded are considered in the present paper: (1) a polymeric matrix (such as epoxy) which is assumed to behave as a linearly elastic material and (2) a metallic matrix (such as aluminum alloy) which is assumed to behave as an elastic-viscoplastic work-hardening material (Bodner, 2002).

In order to utilize the shape memory effect, the composite is activated by an isothermal mechanical loading followed by unloading to a state of overall zero stresses associated with non-zero overall strains. Due to the presence of SMA fibers, a subsequent application of thermal loading to traction-free composite plate reduces the overall residual strains. On the other hand, in a pre-loaded composite plate in which the in-plane displacements of the edges are restrained, the heat induced reduction of the residual strains is prevented and recovery tensile stresses develop. These tensile stresses, caused by the phase transformation, reduce or even overcome the compressive stresses generated by thermal expansion. As a result, the deflection of the plate due to thermal loading is expected to be less than the deflection of the corresponding unactivated plate (namely without pre-loading). Thus the ability to control a structure can be achieved by utilizing the shape memory effect. It is obvious that an activating pre-loading cycle when applied to the active composite, generates internal residual stress and strain fields in the composite constituents. The micromechanical approach enables the incorporation of the effect of these residual micro fields on the structural behavior under the subsequent thermal loading.

Results are presented that exhibit the response of SMA/epoxy and SMA/aluminum composites, as well as that of the monolithic SMA and inelastic aluminum constituents. In particular, the effect of the three-dimensional state of stress that exists in the SMA and matrix phases on the overall composite behavior is shown.

The behavior of plates, consisting of active polymeric matrix and metal matrix composites with embedded SMA fibers, under the sudden application of thermal loading, is shown. To this end, the mechanical loading prior to the application of the thermal load, namely, the activation, is applied to the composite. It is worth mentioning that the transient temperature effects have been taken into account in the macro level of the structural analysis, and a time-dependent dynamic structural behavior is considered.

2. Material behavior

The response of a material that can, in general, exhibit a thermo-elastic-inelastic behavior is governed by the following constitutive law

$$\sigma_{ij} = C_{ijkl}(\varepsilon_{kl} - \varepsilon^{\mathrm{I}}_{kl} - \varepsilon^{\mathrm{T}}_{kl}) \tag{1}$$

where σ_{ij} is the stress tensor, ε_{ij}, $\varepsilon^{\mathrm{I}}_{ij}$, and $\varepsilon^{\mathrm{T}}_{ij} = \alpha_{ij}\Delta T$ are the total, inelastic and thermal strains, respectively, C_{ijkl} is the established stiffness tensor, α_{ij} is the thermal expansion tensor, and ΔT is the temperature deviation from a reference temperature T_{R}. For a perfectly elastic material, $\varepsilon^{\mathrm{I}}_{ij} = 0$.

2.1. Elastic-viscoplastic material

For elastic-viscoplastic material, the inelastic strain rates are controlled by the Prendtl–Reuss flow rule

$$\dot{\varepsilon}^{\mathrm{I}}_{ij} = \Gamma\sigma'_{ij} \tag{2}$$

where Γ is the flow function, $\sigma'_{ij} = \sigma_{ij} - (1/3)\sigma_{kk}\delta_{ij}$ is the deviatoric stress and dot stands for a derivative with respect to time. In the framework of the unified viscoplasticity theory of Bodner and Partom (Bodner, 2002) the function Γ is given by

$$\Gamma = D_0 \exp[-\tilde{n}(Z^2/3J_2)^n]/J_2^{1/2} \tag{3}$$

where $\tilde{n} = (n+1)/2n$, $J_2 = \sigma'_{ij}\sigma'_{ij}/2$, D_0 and n are inelastic material parameters and Z is a state variable representing the work-hardening. For isotropic hardening its rate is given by

$$\dot{Z} = m(Z_1 - Z)\dot{W}_{\mathrm{p}}/Z_0 \tag{4}$$

where Z_0, Z_1 and m are additional material constants, and $\dot{W}_{\mathrm{p}} = \sigma_{ij}\dot{\varepsilon}^{\mathrm{I}}_{ij}$ is the rate of the plastic work.

2.2. Shape memory alloy

The special characteristics of SMA are attributed to microstructural changes affecting the quantitative relations between martensitic and austenitic phases. This process, the phase transformation, is controlled by the evolution of an internal variable ξ that measures the martensitic volume fraction.

Adopting the thermomechanical model of Lagoudas et al. (1996), the transformation strain rate is given by

$$\dot{\varepsilon}^{\mathrm{I}}_{ij} = \Lambda_{ij}\dot{\xi} \tag{5}$$

where

$$\Lambda_{ij} = \begin{cases} \dfrac{3H}{2\overline{\sigma}}\sigma'_{ij}, & \dot{\xi} > 0 \\ \dfrac{H}{\overline{\varepsilon}^{\mathrm{I}}}\varepsilon^{\mathrm{I}}_{ij}, & \dot{\xi} < 0 \end{cases} \tag{6}$$

Here $\overline{\sigma} = [(3/2)\sigma'_{ij}\sigma'_{ij}]^{1/2}$ is the effective stress, $\overline{\varepsilon}^{\mathrm{I}} = [(2/3)\varepsilon^{\mathrm{I}}_{ij}\varepsilon^{\mathrm{I}}_{ij}]^{1/2}$ is the effective transformation strain and $H = \varepsilon^{\mathrm{I}\max}$ is the maximum axial transformation strain.

The stress dependent temperatures at which the forward and reverse martensite–austenite transformations start and finish are

$$\begin{aligned} M^{\mathrm{s}} &= M^{0\mathrm{s}} + \frac{\sigma_{ij}\Lambda_{ij}}{HC^{\mathrm{M}}}, \quad M^{\mathrm{f}} = M^{0\mathrm{f}} + \frac{\sigma_{ij}\Lambda_{ij}}{HC^{\mathrm{M}}} \\ A^{\mathrm{s}} &= A^{0\mathrm{s}} + \frac{\sigma_{ij}\Lambda_{ij}}{HC^{\mathrm{A}}}, \quad A^{\mathrm{f}} = A^{0\mathrm{f}} + \frac{\sigma_{ij}\Lambda_{ij}}{HC^{\mathrm{A}}} \end{aligned} \tag{7}$$

with $M^{0\mathrm{s}}, M^{0\mathrm{f}}, A^{0\mathrm{s}}, A^{0\mathrm{f}}$ being the martensitic start, martensitic finish, austenitic start and austenitic finish temperatures under stress-free state, respectively. The material constants $C^{\mathrm{M}}, C^{\mathrm{A}}$ are the martensitic and austenitic stress influence coefficients.

The state equation for the martensitic volume fraction is

$$\dot{\xi} = -\frac{(R_{ij}\dot{\varepsilon}_{ij} + S\dot{T})}{B} \tag{8}$$

where

$$\begin{aligned} R_{ij} &= C_{ijkl}\frac{\partial \Phi}{\partial \sigma_{ij}} \\ S &= \frac{\partial \Phi}{\partial T} - \frac{\partial \Phi}{\partial \sigma_{ij}}C_{ijkl}\alpha_{kl} \\ B &= \frac{\partial \Phi}{\partial \sigma_{ij}}P_{ij} + \frac{\partial \Phi}{\partial \xi} \\ P_{ij} &= \frac{\partial \sigma_{ij}}{\partial \xi} \\ a^{\mathrm{M}} &= \frac{\ln(0.01)}{(M^{\mathrm{s}} - M^{\mathrm{f}})} \\ a^{\mathrm{A}} &= \frac{\ln(0.01)}{(A^{\mathrm{s}} - A^{\mathrm{f}})} \end{aligned} \tag{9}$$

and the function Φ is given by

$$\Phi = \begin{cases} \sigma_{ij}\Lambda_{ij} + HC^{\mathrm{M}}\left(M^{0\mathrm{s}} - T - \dfrac{\ln(1-\xi)}{a^{\mathrm{M}}}\right), & \dot{\xi} > 0, \;\; M^{\mathrm{f}} \leqslant T \leqslant M^{\mathrm{s}} \\ -\sigma_{ij}\Lambda_{ij} - HC^{\mathrm{A}}\left(A^{0\mathrm{s}} - T - \dfrac{\ln(\xi)}{a^{\mathrm{A}}}\right), & \dot{\xi} < 0, \;\; A^{\mathrm{s}} \leqslant T \leqslant A^{\mathrm{f}} \end{cases} \tag{10}$$

2.3. Unidirectional composite

Consider an active composite material which consists of SMA fibers embedded in a metallic or polymeric matrix. The effective mechanical and thermal behavior of the unidirectional composite is determined by a micromechanical analysis referred to as the generalized method of cells (Paley and Aboudi, 1992; Aboudi,

1996). In the framework of this method, the overall composite constitutive law is obtained in terms of the elastic and inelastic material properties of the constituents and their detailed interaction. Expressed with respect to material coordinates, one of which (the 1-direction) coincides with the fiber direction, the overall constitutive relations that control the composite global behavior is given by

$$\sigma_{ij} = C^*_{ijkl}(\varepsilon_{kl} - \varepsilon^{\mathrm{I}}_{kl} - \varepsilon^{\mathrm{T}}_{kl}), \quad i,j,k,l = 1,2,3 \tag{11}$$

Here C^*_{ijkl} is the overall elastic stiffness tensor of the composite, σ_{ij}, ε_{ij} and $\varepsilon^{\mathrm{I}}_{ij}$ are the average stress, the average total strain and the composite inelastic strain tensors, respectively. The thermal strain of the composite is $\varepsilon^{\mathrm{T}}_{ij} = \alpha^*_{ij}\Delta T$ where α^*_{ij} is the effective thermal expansion tensor.

It should be noted that extensive verifications of the micromechanical analysis under various circumstances have been carried out by many investigators as is summarized in the review paper by Aboudi (1996).

3. Structural behavior

Consider a laminated rectangular plate of an infinite width in the y direction, uniformly supported along the edges $x = 0, L$, at a state of initial uniform reference temperature T_{R}. The thickness of the plate is h and the coordinate z is perpendicular to the plane of the plate with its origin placed in the mid-plane. The plate is subjected to a surface thermal loading.

In the framework of the classical plate theory, the von-Karman strains are given by

$$\begin{aligned} \varepsilon_{xx} &= \varepsilon^0_{xx} + z\varepsilon^1_{xx} \\ \varepsilon_{xy} &= \varepsilon^0_{xy} \end{aligned} \tag{12}$$

where

$$\varepsilon^0_{xx}(x,t) = u_{x,x} + \frac{1}{2}u^2_{z,x} + u_{z,x}u_{z0,x}$$

$$\varepsilon^0_{xy}(x,t) = \frac{1}{2}u_{y,x}$$

$$\varepsilon^1_{xx}(x,t) = -u_{z,xx}$$

and u_x, u_y, u_z denote the displacements of a point on the mid-plane, and $u_{z0} = w_0 h \sin(\pi x/L)$ is the initial geometrical imperfection. Comma is used for denoting spatial derivatives.

The force and moment resultants are given by

$$(N_{ij}, M_{ij}) = \int_{-\frac{h}{2}}^{\frac{h}{2}} \sigma_{ij}(1,z)\,\mathrm{d}z \quad i,j = x,y \tag{13}$$

For a plane-stress state, these definitions yield the following plate constitutive relations

$$\begin{bmatrix} N_{xx} \\ N_{xy} \\ M_{xx} \end{bmatrix} = \begin{bmatrix} A_{11} & A_{16} & B_{11} \\ A_{16} & A_{66} & B_{16} \\ B_{11} & B_{16} & D_{11} \end{bmatrix} \begin{bmatrix} \varepsilon^0_{xx} \\ 2\varepsilon^0_{xy} \\ \varepsilon^1_{xx} \end{bmatrix} - \begin{bmatrix} N^{\mathrm{I}}_{xx} \\ N^{\mathrm{I}}_{xy} \\ M^{\mathrm{I}}_{xx} \end{bmatrix} - \begin{bmatrix} N^{\mathrm{T}}_{xx} \\ N^{\mathrm{T}}_{xy} \\ M^{\mathrm{T}}_{xx} \end{bmatrix} \tag{14}$$

where the extension, coupling and bending stiffness matrices A_{ij}, B_{ij}, D_{ij} are defined as usual

$$\left(A_{ij}, B_{ij}, D_{ij}\right) = \int_{-\frac{h}{2}}^{\frac{h}{2}} Q_{ij}\left(1, z, z^2\right)\mathrm{d}z \quad i,j = 1,2,6 \tag{15}$$

where Q_{ij} are the reduced effective stiffness coefficients defined with respect to the plate coordinates system (x,y,z). If the material coordinates system is rotated through an angle θ about a coordinate coinciding with

the plate's coordinate z, the coefficients Q_{ij} are obtained from the corresponding quantities in the overall constitutive law, Eq. (11), by a transformation from the material coordinates to the plate coordinates.

The inelastic forces and moments are given by

$$\begin{aligned}\left(N_{xx}^{\mathrm{I}}, M_{xx}^{\mathrm{I}}\right) &= \int_{-\frac{h}{2}}^{\frac{h}{2}} \left[Q_{11}\varepsilon_{xx}^{\mathrm{I}} + Q_{12}\varepsilon_{yy}^{\mathrm{I}} + Q_{16}2\varepsilon_{xy}^{\mathrm{I}}\right](1, z)\,\mathrm{d}z \\ \left(N_{xy}^{\mathrm{I}}\right) &= \int_{-\frac{h}{2}}^{\frac{h}{2}} \left[Q_{16}\varepsilon_{xx}^{\mathrm{I}} + Q_{26}\varepsilon_{yy}^{\mathrm{I}} + Q_{66}2\varepsilon_{xy}^{\mathrm{I}}\right](1)\,\mathrm{d}z\end{aligned} \tag{16}$$

The thermal forces and moments are given by

$$\begin{aligned}\left(N_{xx}^{\mathrm{T}}, M_{xx}^{\mathrm{T}}\right) &= \int_{-\frac{h}{2}}^{\frac{h}{2}} \left[Q_{11}\alpha_{xx} + Q_{12}\alpha_{yy} + Q_{16}2\alpha_{xy}\right]\Delta T(1, z)\,\mathrm{d}z \\ \left(N_{xy}^{\mathrm{T}}\right) &= \int_{-\frac{h}{2}}^{\frac{h}{2}} \left[Q_{16}\alpha_{xx} + Q_{26}\alpha_{yy} + Q_{66}2\alpha_{xy}\right]\Delta T(1)\,\mathrm{d}z\end{aligned} \tag{17}$$

The governing equations of motion of the infinitely wide plate are (Reddy, 1997)

$$\begin{aligned}&N_{xx,x} = I\ddot{u}_x \\ &N_{xy,x} = I\ddot{u}_y \\ &M_{xx,xx} + \left[N_{xx}(u_{z,x} + u_{0z,x})\right]_{,x} = I\ddot{u}_z\end{aligned} \tag{18}$$

where $I = \int_{-\frac{h}{2}}^{\frac{h}{2}} \rho\,\mathrm{d}z$, with ρ being the effective mass density of the composite.

These governing equations of motion are associated with initial and boundary conditions. For a plate being at rest at time $t = 0$ when loading commences, the initial conditions are

$$\begin{aligned}&u_x = u_y = u_z = 0 \\ &\dot{u}_x = \dot{u}_y = \dot{u}_z = 0 \quad \text{at} \quad t = 0,\ \ 0 \leqslant x \leqslant L\end{aligned} \tag{19}$$

The boundary conditions at $x = 0$ and $x = L$ have the form

$$u_x = u_y = u_z = M_{xx} = 0 \quad \text{at} \quad t > 0 \tag{20}$$

for the case of simply supported edges. These boundary conditions imply constraints on both in-plane and out-of-plane displacements along the boundaries.

By substituting the plate constitutive relations in conjunction with the strain–displacement relations into the equations of motion, a set of nonlinear partial differential equations in terms of the displacements components is obtained. Central differences of the spatial derivatives in these equations leads to a system of difference equations which forms an initial value problem, that can be solved by the Runge–Kutta method. This is performed in conjunction with an incremental procedure that follows the development of inelasticity. Namely, at the end of each time interval and at every point of the structure, the aforementioned micromechanical analysis is employed in order to predict the inelastic strain rates and the local state variables. Assuming that these values remain constant during the following time increment, the instantaneous values of the structure stiffness matrices, inelastic and thermal forces and moments are then calculated from (15)–(17), by performing the integration along z numerically. Convergence is ensured by choosing sufficiently small spatial and time increments.

4. Application

In order to verify the accuracy of the micromechanical analysis prediction in the presence of SMA fibers and elastic matrix, comparison with the results of Boyd and Lagoudas (1994) have been performed and excellent agreement was found. In the case a SMA fibers reinforcing inelastic aluminum matrix, comparison with the finite element results of Lagoudas et al. (1994) have been performed and good agreement have been obtained (taking into account the different approaches for the modelling of the inelastic phase).

In the following, results are presented that exhibit the response of the SMA material, aluminum matrix, SMA/Al and SMA/epoxy. In addition, the behavior of active composite plates subjected to thermal loading is presented.

4.1. Unidirectional composite response

The material behavior of composites with embedded SMA fibers is investigated. The material constants are assumed to be temperature independent, and are given in Table 1. In all cases, a fiber volume fraction 0.3 is considered.

The great advantage of the use of SMA material stems from the fact that it can be employed as an actuator. This is due to its ability, under certain circumstances, to reduce by a temperature increase the residual strains which have been generated by a pre-applied mechanical loading. However, if during such heating the reduction of these residual strains is prevented by an external mean, recovery stresses develop. These stresses can be employed to control the behavior of the structure.

In Fig. 1, the uniaxial stress–strain behavior in the 1-direction of the SMA fibers, inelastic aluminum matrix and the SMA/Al unidirectional composite are shown. These behaviors are shown at different temperatures because the SMA constituent exhibits different temperature-dependent responses. At temperature $T = 25$ °C, which is lower than the austenitic start temperature, the residual strain obtained after the first unloading to zero stress is rather significant. At a higher temperature $T = 35$ °C, which is higher than the austenitic start temperature and lower than the austenitic finish temperature, the residual strain decreases. This residual strain vanishes at $T = 55$ °C which is above the austenitic finish temperature at which the SMA exhibits superelastic behavior. It is clearly seen from Fig. 1 that the inelastic matrix (whose response is exhibited in Fig. 1(d)) has a dominant role on the composite behavior. In particular, in the presence of the inelastic matrix, residual strains are obtained after the first unloading to zero stress at all those temperatures. This has a significant effect on the composite behavior when subjected to a subsequent thermal cycle.

Table 1
Material constants

	Epoxy	Aluminum	SMA
E (GPa)	3.45	69.0	21.5
v	0.35	0.33	0.33
ρ (kg/m^3)	1218	2700	6700
α (10^{-6}/°C)	20.0	23.1	8.8
k (W/m °C)	0.18	180.0	56.5
c (Ws/kg °C)	921.0	840.0	528.5
		$D_0 = 10,000$/s	$M^{0f} = 5$ °C, $M^{0s} = 23$ °C
		$Z_0 = 52$ MPa	$A^{0s} = 29$ °C, $A^{0f} = 51$ °C
Inelastic constants		$Z_1 = 135$ MPa	$C^M = 11.3$ MPa/°C
		$m = 31$	$C^A = 4.5$ MPa/°C
		$n = 10$	$H = 0.0423$

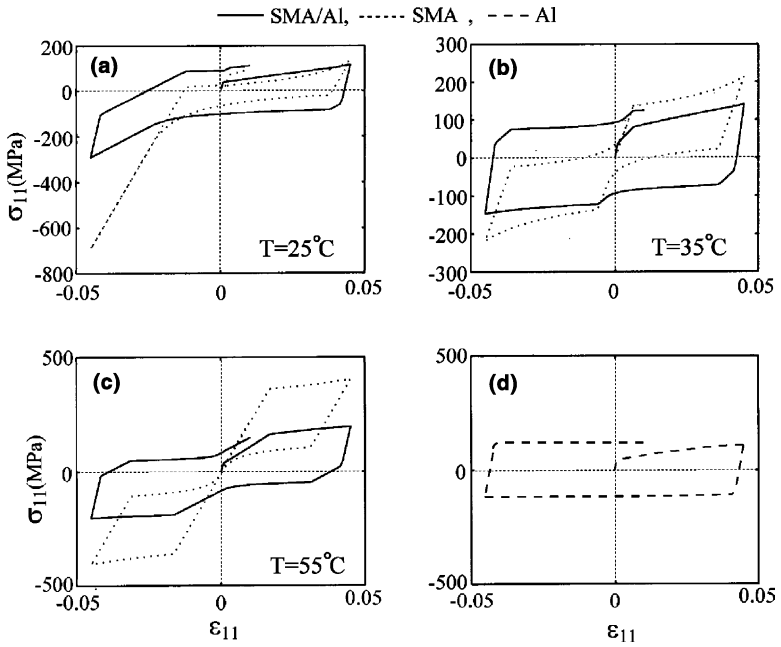

Fig. 1. Uniaxial stress–strain response in the 1-direction of SMA, Al and SMA/Al composite.

It is interesting to examine the interaction between the SMA constituent and an elastic resin matrix. Fig. 2 presents the uniaxial stress–strain response in the 1-direction of SMA/epoxy composite and the monolithic SMA material at the same temperature values that have been discussed in Fig. 1. Due to the absence of the inelastic mechanism and the lower value of Young's modulus of epoxy as compared with that of the SMA, the effect of the latter on the overall composite behavior is dominant.

In both Figs. 1 and 2, the loading has been applied in the 1-direction in which the SMA fibers are oriented. Fig. 3 illustrates the behavior of the SMA/Al and SMA/epoxy when the loading is applied in the

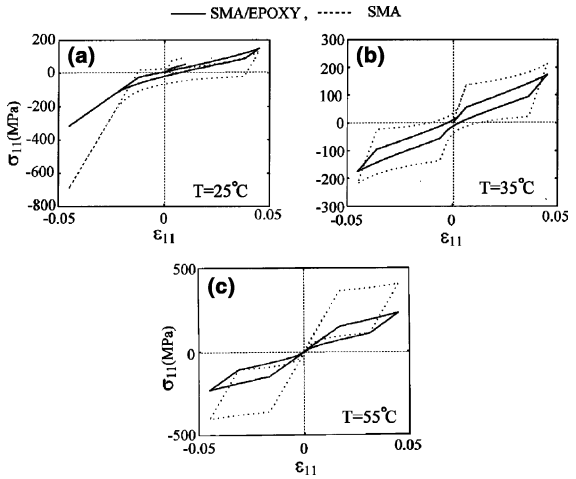

Fig. 2. Uniaxial stress–strain response in the 1-direction of SMA and SMA/epoxy composite.

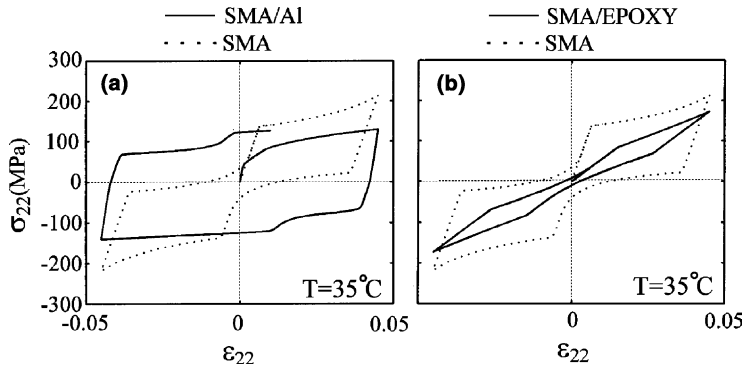

Fig. 3. Uniaxial stress–strain response in the 2-direction of SMA/Al and SMA/epoxy composite.

transverse 2-direction perpendicular to the fibers. It can be readily seen that in the case of metal matrix composite minor differences are detected when the loading is applied either in the fiber direction or perpendicular to the fibers. In the case of the resin matrix composite, one can observe that the initial elastic slope of the composite, as can be expected, is lower in the transverse loading case. In the inelastic region of the SMA constituent however, the global response of the composite is still dominated by the latter behavior as in the case of axial loading.

In order to demonstrate the ability of the embedded SMA material to control the composite response, it is necessary to examine the behavior due to a mechanical loading-unloading, followed by a temperature increase. Fig. 4 shows the response in the 1-direction of the unidirectional SMA/Al composite and the SMA material both subjected to uniaxial stress loading-unloading at $T = T_R = 35$ °C, followed by a temperature increase under traction-free conditions. The shape memory effect in the SMA material, which is exhibited by the decrease of the strain due to the temperature increase, is clearly observed. This effect is caused by the phase transformation which depends, in general, on the temperature and stress state. Under traction-free situation this transformation starts together with the temperature increase as is seen in Fig. 4. The

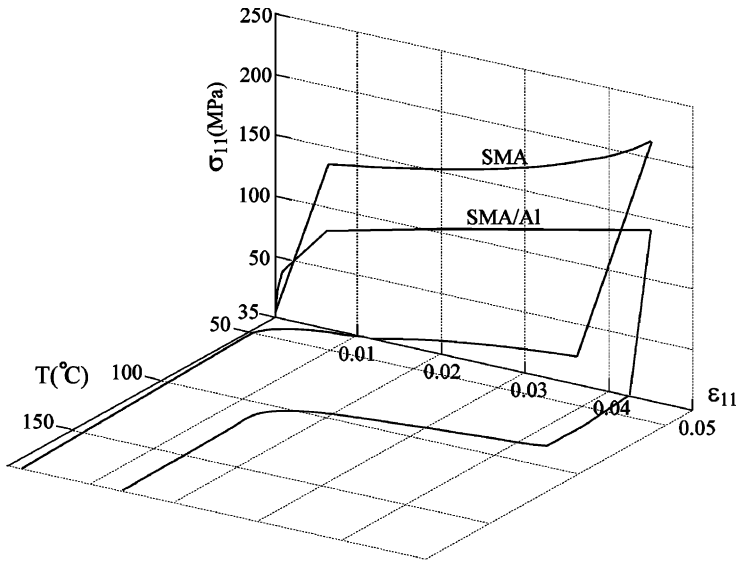

Fig. 4. Stress–strain–temperature response of SMA and SMA/Al composite exhibiting the strain recovery.

transformation process is completed at the austenitic finish temperature $T = A^{0f} = 51$ °C where the strain is very small. Further heating induces a slight strain increase due to the thermal expansion of the SMA material. Similar process takes place in the SMA/Al composite. Here however, since the SMA constituent is subjected to residual stresses, the phase transformation which is accompanied by an overall strain reduction starts at a higher temperature (about 80 °C). Further heating decreases the residual overall strain. This strain reduction is more significant that the strain reduction that takes place in the monolithic SMA constituent.

As stated before, constraining the composite by preventing the strain reduction, yields significant recovery stresses. Fig. 5 illustrates the effect of the recovery stresses. It shows the behavior of the monolithic SMA and composite due to axial mechanical loading-unloading, followed by heating under the constraint of constant axial strain. The beginning of the phase transformation in the composite is reflected by the slope change in the stress–temperature plane.

4.2. Structural response

The behavior of infinitely wide plates consisting of unidirectional SMA/Al or SMA/epoxy composites and subjected to the sudden application of a thermal loading is studied. The abrupt change in the temperature induces inertia effects that are accounted for by the terms on the right-hand sides of Eq. (18). A thickness ratio of $L/h = 100$ is considered, and the response of the plate is presented by the time variation of the dimensionless maximum out-of-plane displacement $\overline{w} = \max_x |u_z|/h$.

Neglecting the thermomechanical coupling, the temperature field in the plate satisfies the Fourier heat conduction equation.

$$-(k_{ij}T_{,j})_{,i} + \rho c\dot{T} = 0 \tag{21}$$

where k_{ij} is effective thermal conductivity and c is the effective specific heat of the composite. In the following, two solutions of the heat conduction equation which are given by Carslaw and Jaeger (1960) are used to describe the temperature distribution throughout the plate's thickness.

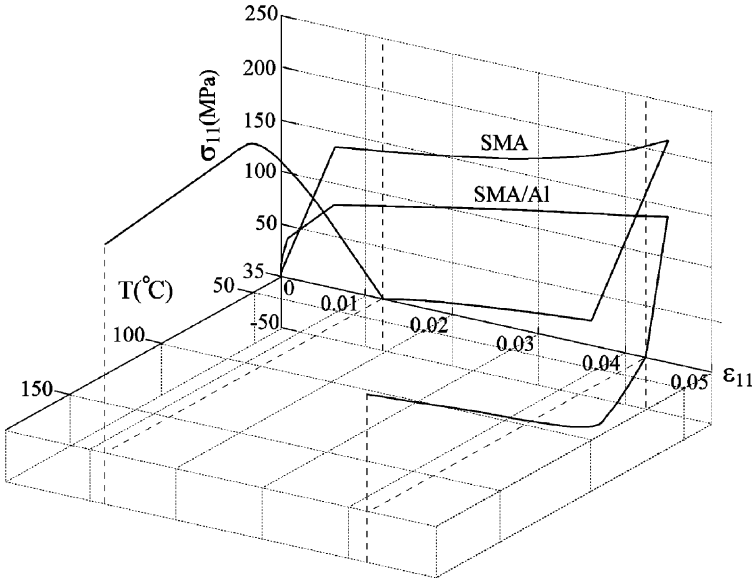

Fig. 5. Stress–strain–temperature response of SMA and SMA/Al composite exhibiting the stress recovery.

For the case of a uniform heat flux q_0 suddenly applied to the upper surface $z = h/2$ while the lower surface $z = -h/2$ is kept perfectly insulated, the temperature variation is

$$\Delta T(z,t) = \frac{q_0 t}{\rho c h} + \frac{q_0 h}{k_z}\left[\frac{1}{2}\left(\frac{z}{h}+\frac{1}{2}\right)^2 - \frac{1}{6} - \frac{2}{\pi}\sum_{p=1}^{\infty}\frac{(-1)^p}{p^2}\mathrm{e}^{-\kappa_z p^2\pi^2 t/h^2}\cos\left(p\pi\left(\frac{z}{h}+\frac{1}{2}\right)\right)\right] \tag{22}$$

where $\kappa_z = k_z/\rho c$ is the effective thermal diffusivity.

If both surfaces of the plate, being initially at a temperature T_R, are subjected to the following temperature increase

$$T = T_\mathrm{R} + T_\mathrm{m}(1-\mathrm{e}^{-\beta t}), \quad t > 0,\ z = \pm\frac{h}{2} \tag{23}$$

such that the maximum value of the temperature change is T_m (β is a parameter), the resulting distribution of the temperature change through the thickness is

$$\Delta T(z,t) = T_\mathrm{m}\left[1 - \frac{\cos(z^2\beta/\kappa_z)^{\frac{1}{2}}}{\cos(h^2\beta/4\kappa_z)^{\frac{1}{2}}}\mathrm{e}^{-\beta t} - \frac{16\beta h^2}{4\pi}\sum_{p=0}^{\infty}\frac{(-1)^p\mathrm{e}^{-\kappa_z(2p+1)^2\pi^2 t/h^2}}{(2p+1)[\beta h^2 - \kappa_z\pi^2(2p+a)^2]}\cos\frac{(2p+1)\pi z}{h}\right] \tag{24}$$

As this temperature distribution is symmetric with respect to $z = 0$, an initial imperfection with $w_0 = 0.01$ is included in order to get non-zero transverse displacements of a unidirectional plate.

In order to illustrate the shape memory effect on the composite structure behavior, two separate situations are considered. In the first one the SMA fibers have been activated through a cycle of mechanical loading-unloading applied to the composite, which gives rise to a residual global strain associated with overall traction-free state. In the present investigation this activation procedure involves loading to a stain of 0.045. This pre-loading enables the realization of the shape memory effect during a subsequent thermal loading. The second situation exhibits the behavior of the same structure but without the pre-loading procedure.

Figs. 6 and 7 show the response of a [0°] (fiber oriented in the x direction) wide plate, kept initially at a temperature $T_\mathrm{R} = 35$ °C, subjected to a heat flux of low and high amplitudes, respectively, at the upper surface, while keeping the lower surface insulated. The inserts to the figures show the temperature distribution through the plate's thickness, given by Eq. (22), at different times. Since the case of low heat flux amplitude induces a slow and uniform through the thickness temperature increase in the plate, it corresponds to a quasi-static loading. The high amplitude value, on the other hand is associated with a non-uniform rapid increase of temperature, implying a dynamic situation. The curve of the activated plate in Fig. 6 clearly shows the start and finish points of the SMA phase transformation. The start of the transformation is associated with a reduction of the axial resultant force and a significant change in the development of the out-of-plane displacement. At the end of the transformation process there is a rapid increase in deflection, yet it remains lower than in the unactivated case. In the rapid heating case of Fig. 7 one can still observe the start and finish points of the SMA phase transformation. However the presence of the dynamic effects introduces oscillations and reduces the effect of the activation.

Whereas in Figs. 6 and 7 the temperature in the plate keeps increasing, it should be interesting to examine the case of a temperature that suddenly rises to a constant value as described by Eq. (23) and the insert to Fig. 8. The resulting temperature distribution is given by Eq. (24). The response of the [0°] plate is shown in Fig. 8 where, though the observed oscillations indicate appreciable dynamic effects, a significant influence of the activation is exhibited.

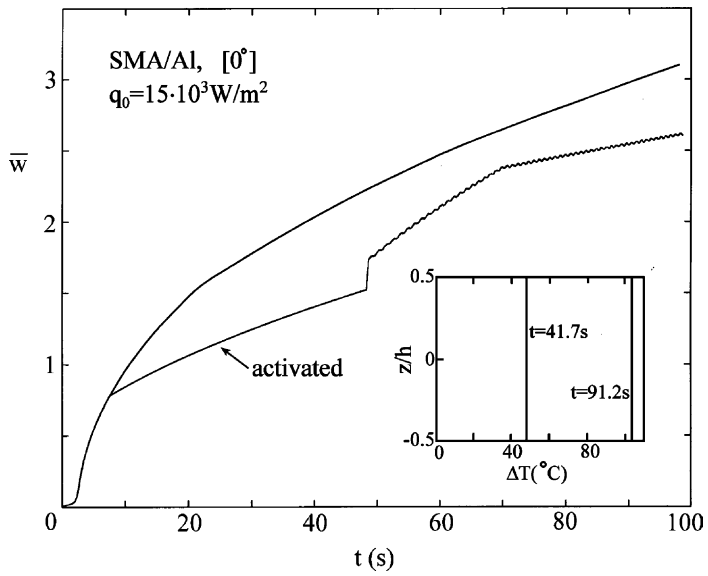

Fig. 6. Variation with time of the out-of-plane displacement of SMA/Al, [0°] plate subjected to a low amplitude heat flux.

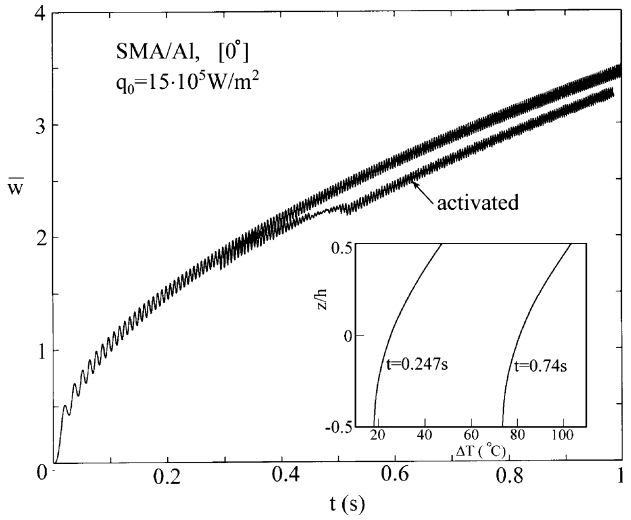

Fig. 7. Variation with time of the out-of-plane displacement of SMA/Al, [0°] plate subjected to a high amplitude heat flux.

For antisymmetric angle-ply $[45°/-45°]$ SMA/Al plate subjected to the aforementioned thermal loading, Eq. (23), on both surfaces, the variation with time of the out-of-plane displacement is shown in Fig. 9. Here it turns out that the activation procedure increases the plate deflection in comparison to the unactivated plate. This implies that in the present situation the activation may be deficient. It should be noted however that under loading of lower amplitudes the curves of activated and unactivated plates approach each other.

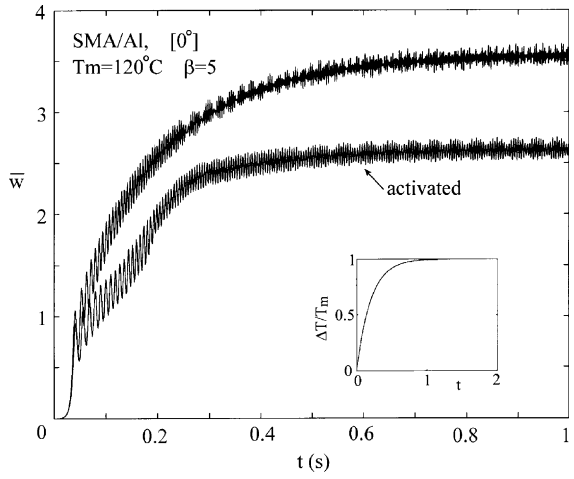

Fig. 8. Variation with time of the out-of-plane displacement of SMA/Al, [0°] plate subjected to a temperature loading.

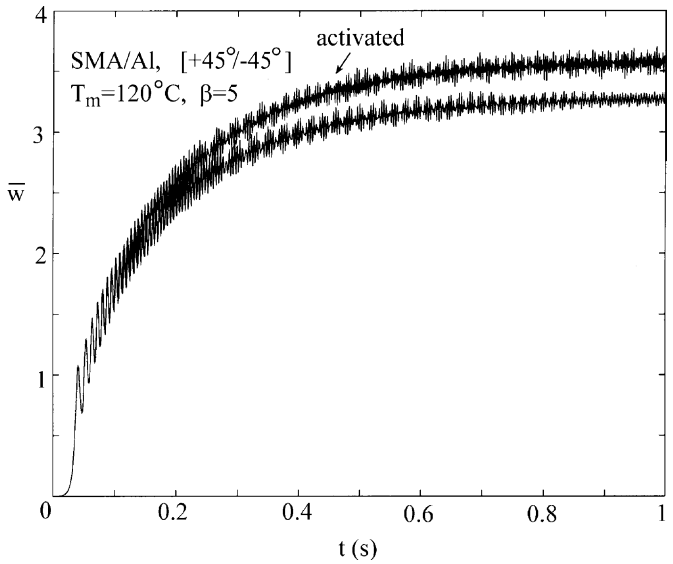

Fig. 9. Variation with time of the out-of-plane displacement of SMA/Al, [45°/−45°] plate subjected to a temperature loading.

The corresponding cases to Figs. 8 and 9 are shown in Figs. 10 and 11 for plates that are composed of SMA/epoxy materials, and are initially kept at a temperature $T_R = 25$ °C. A comparison between Figs. 8 and 10 and between Figs. 9 and 11 shows that the responses of the activated SMA/epoxy plates deviate from the unactivated ones immediately after $t = 0$. This indicates that the phase transformation which generates the shape memory effect in the SMA/epoxy plate starts as soon as heating commences, such that under the present circumstances the efficiency of the activation dramatically increases.

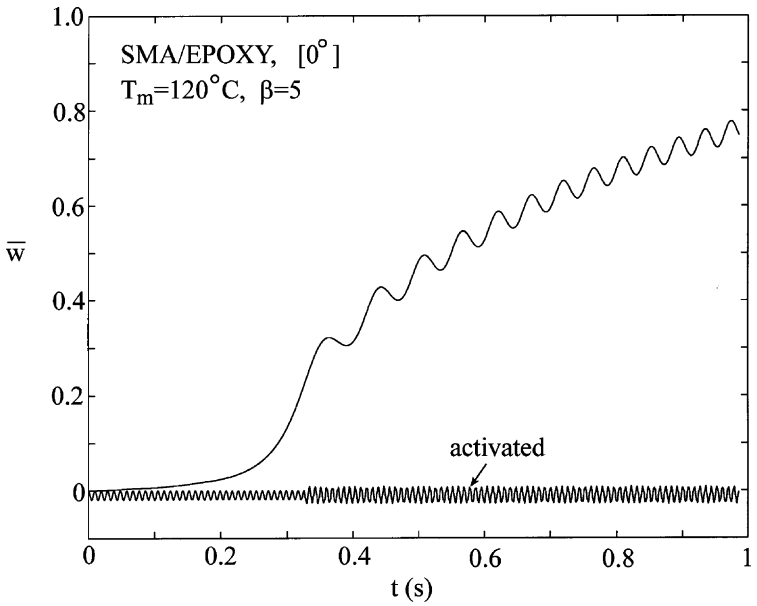

Fig. 10. Variation with time of the out-of-plane displacement of SMA/epoxy [0°] plate subjected to a temperature loading.

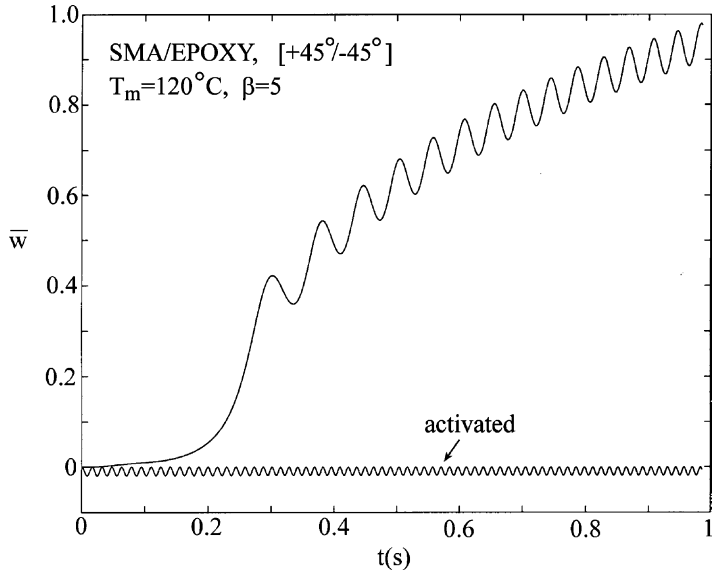

Fig. 11. Variation with time of the out-of-plane displacement of SMA/epoxy [45°/−45°] plate subjected to a temperature loading.

5. Conclusions

A micro-macro-structural approach is offered to predict the capability of SMA fibers embedded in composite plates to control their response. Both polymeric and metallic matrices have been considered in

the present investigation and the detailed interaction between the various constituents is accounted for. The present approach can be generalized to investigate 'smart' composite plates and shells under various loading conditions, and control their response, buckling and post buckling.

Acknowledgements

The second author gratefully acknowledges the support of the Diana and Arthur Belfer chair of Mechanics and Biomechanics.

References

Aboudi, J., 1996. Micromechanical analysis of composites by the method of cells—update. Appl. Mech. Rev. 49, S83–S91.

Auricchio, F., Taylor, R.L., Lubliner, J., 1997. Shape memory alloy macromodelling and numerical simulations of the superelastic behavior. Comput. Methods Appl. Mech. Eng. 146, 281–312.

Bednarcyk, B.A., Arnold, S.M., 2002. MAC/GMC 4.0 User's Manual. NASA/TM-2002-212077.

Birman, V., 1997. Review of mechanics of shape memory alloy structures. Appl. Mech. Rev. 50, 629–645.

Bodner, S.R., 2002. Unified Plasticity for Engineering Applications. Kluwer, New York.

Boyd, J.G., Lagoudas, D.C., 1994. Thermomechanical response of shape memory composites. J. Intell. Mater. Syst. Struct. 5, 333–346.

Brocca, M., Brinson, L.C., Bazant, Z.P., 2002. Three-dimensional constitutive model for shape memory alloy based on microplane model. J. Mech. Phys. Solids 50, 1051–1077.

Carslaw, H.S., Jaeger, J.C., 1960. Conduction of Heat in Solids, second ed. Clarendon Press.

Cherkaoui, M., Sun, Q.P., Song, G.Q., 2000. Micromechanics modelling of composite with ductile matrix and shape memory alloy reinforcement. Int. J. Solids Struct. 37, 1577–1594.

Herakovich, C.T., 1998. Mechanics of Fibrous Composites. Wiley, New York.

Kawai, M., Ogawa, H., Baburaj, V., Koga, T., 1996. Micromechanical analysis for hysteretic behavior of unidirectional TiNi SMA fiber composite. J. Intell. Mater. Syst. Struct. 10, 14–28.

Lagoudas, D.C., Bo, Z., Qidwai, M.A., 1994. Micromechanics of active metal matrix composite with shape memory alloy fibers. In: Voyiadjis, G.Z., Ju, J.W. (Eds.), Inelasticity and Micromechanics of Metal Matrix Composite. Elsevier, New York, pp. 163–190.

Lagoudas, D.C., Bo, Z., Qidwai, M.A., 1996. A unified thermodynamic constitutive model for SMA and finite element analysis of active metal matrix composites. Mech. Compos. Mater. Struct. 3, 153–179.

Lee, H.J., Lee, J.J., 2000. A numerical analysis of the buckling and postbuckling behavior of laminated composite shells with embedded shape memory alloy wires actuators. Smart Mater. Struct. 9, 780–787.

Paley, M., Aboudi, J., 1992. Micromechanical analysis of composites by the generalized cells model. Mech. Mater. 14, 127–139.

Reddy, J.N., 1997. Mechanics of Laminated Composite Plates. CRC Press, Boca Raton.

Tawfik, M., Ro, J.J., Mei, C., 2002. Thermal post-buckling and aeroelastic behavior of shape memory alloy reinforced plates. Smart Mater. Struct. 11, 297–307.

Turner, T.L., 2000. A new thermoelastic model for analysis of shape memory alloy hybrid composites. J. Intell. Mater. Syst. Struct. 11, 382–394.